



3D electrical resistivity forward modeling using the Kirchhoff's method for solving an equivalent resistor network

Arshia Gerami

Universiti Teknologi Petronas, Malaysia

ARTICLE INFO

Article history:

Received 29 March 2017

Received in revised form 28 January 2018

Accepted 9 August 2018

Available online 23 August 2018

Keywords:

Geophysics

Geoelectric

Resistivity

Kirchhoff

Forward modeling

ABSTRACT

There are different approaches to solve the three-dimensional (3D) resistivity model. In this research, a new modeling technique has been developed to solve 3D potential distribution in a resistor network. This method uses the Kirchhoff's law for discretizing a resistor network. This different approach for the 3D resistivity modeling helps to describe an arbitrary 3D model using a resistor network. This method has no singularity constraint, although there is no need to apply any singularity removal techniques. The resistor network can be used for any electrode configuration. The potential distributions at all nodes are simultaneously solved for each injection source. Sensitivity matrix and potential distribution in both models are compared.

Experiments with various physical models and numerical models show the similarity of the method with traditional resistivity modeling. Comparing the result of this approach with other methods shows better sensitivity away from edges. Furthermore, a parallel programming technique is used to improve the processing time. Flexibility and extensibility to build any resistivity model make this approach a powerful modeling tool in 2D and 3D electrical resistivity forward modeling.

© 2018 Elsevier B.V. All rights reserved.

1. Introduction

Electrical resistivity forward modeling is used for calculating the potential distribution in a model. There are different numerical techniques for doing so since Dey and Morrison (1979) introduced a computerized finite difference method for solving arbitrary shapes. Zhang et al. (1995) introduced a model with a resistor network, and used it for the forward modeling section in their research, in which they solved the model with a similar concept. Since then, there have been different approaches to solve this problem such as Loke and Dahlin conjugate gradient and quasi-newton Loke and Dahlin (2002) to improve either accuracy or speed.

These numerical methods were applied by Dahlin and Zhou (2004), to calculate the model results for 10 different electrode configurations, and also for different multi-electrode arrays by Martorana et al. (2009). With improvement of computers and numerical methods, finite difference and finite element are used widely to solve the same model. Wilkinson et al. (2006) used finite difference algorithm for their tomography studies Wilkinson et al. (2006), Wilkinson et al. (2012), also Plattner et al. (2012). Loke et al. (2010a, 2010b) used the finite difference method as a core for solving optimization problems Loke et al. (2010a, 2010b), Loke et al. (2014b). There are also several outstanding researches on finite difference methods such as Mufti (1976), Spitzer

(1995), Wang et al. (2000). Sasaki (1994) solved this problem using finite element method Sasaki (1989). There are other papers in this area such as Coggon (1971), Bing and Greenhalgh (2001) and Li and Spitzer (2002). There are other methods as the boundary elements method (BEM) by Hvozda and Kaikkonen (1998), Xu et al. (1998) and Ma (2002) as well. Integral equation methods (IEM) is another approach for solving this problem as Lee (1975), Dieter et al. (1969).

The method used in this paper is similar to creating a wireframe model. So it can be applied to any shape. Though any topography will be handled with this approach, it is similar to Penz et al. (2013). Furthermore, changing the resistor value enables this method, to handle any anisotropic distribution of electrical properties such as dikes. Also by modifying resistor values in the resistor network, the affects of long electrodes Rucker et al. (2010) or electrical borehole modeling could be simulated as Loke et al. (2014a). Finally, extending boundary will give more accurate modeling results.

In this article, a noble modeling approach for 3D resistivity modeling is presented. This method helps to describe an arbitrary 3D model using a resistor network and applies the Kirchhoff's Law to solve the model. This resistor network is similar to the resistivity model for comparison purposes.

Resistor network could be a better solution for studying a physical model built by resistors because the results are exact. Removing singularity in electrical resistivity forward modeling is an advanced technique as it is explained by Lowry et al. (1989), which is not necessary in this method as there is no singularity after the main matrix is formed. This

E-mail address: arshia.gerami@gmail.com.

feature does not only make the solving simpler but makes the procedure steps easier.

There are more attributes in the resistor network models as they are distributed in the edges rather than the center. This makes modeling more detailed. This technique can be used in conventional or unconventional methods with the same procedure in order to reduce complexity. The final result will be a system of linear equations without any complications or singularity problems. Solving this system of linear equations will provide the model response. Finally, a parallel programming method, using NVIDIA graphic card functionality is used to dramatically improve the processing time needed to solve the linear system of equations.

2. Theory

3D modeling of the earth model using a resistor network makes modeling easier and more robust, especially when it comes to calculating models like tanks or resistor networks. Application of the Kirchhoff's Law and nodal analysis helps to model this resistor network more efficiently. It uses the Kirchhoff's Current Law (KCL¹) and the Kirchhoff's Voltage Law (KVL²) for analyzing the model. This method, considers the earth as a cube of wires with each edge as a resistor, rather than a resistor block. As such, this method can give the user more flexibility to study the model in more detail while the model response to different electrode configurations remains the same.

In this method, the center of the cube is shifted to the corners; these centers will represent the cube nodes, all connected within a resistor as shown in Fig. 1. Each resistivity cube is changed to a wire framed resistor while the nodes for electrodes remain in the same position in both models. As these cubes fundamentally are different (one is resistivity with ohm-meter unit and the other is resistor with ohm unit) the measurement for distance unit is chosen 1 to avoid confusion.

Also changing the resistor values can shape the topography, or play the role of the long electrode; which will be discussed later. In geoelectrics most researchers use the Dey method for discretizing their matrix. In this paper, the Kirchhoff's Law has been used directly to discretize the resistor network, which will be explained later. By applying this method to a well-known resistivity problem, and to the whole matrix formulation; the approach for analyzing the model will fundamentally change.

2.1. Fundamental relations

In this section the formulation of both methods (discretizing with the Dey method and the Kirchhoff's Law) are presented and the similarities and differences are discussed.

Assume there is a 3D medium, and it has an anomaly in (x, y, z) as shown in Fig. 1. Based on Ohm's Law we have:

$$\vec{J} = \sigma \vec{E} \quad (1)$$

where \vec{J} is the current density, \vec{E} is electrical field intensity and σ is an isotropic conductivity. Since static electric field is conservative:

$$\vec{E} = -\nabla \phi_{(x,y,z)} \quad (2)$$

where ϕ is the electrical potential.

¹ Kirchhoff's Current Law is the Kirchhoff's first law which defines the sum of all currents that enter an electrical circuit junction is 0

² Kirchhoff's Voltage Law is the Kirchhoff's second law which defines the sum of all voltages or potential differences in an electrical circuit loop is 0.

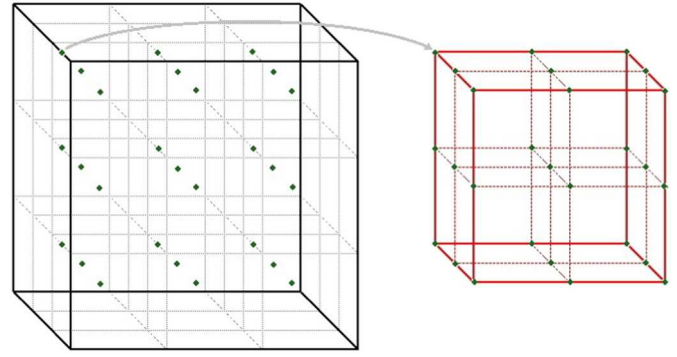


Fig. 1. Resistivity model.

Applying the principle of conservation of charge over a volume and using the equation of continuity should obtain:

$$\nabla \cdot \vec{J} = I \delta(x-x_p) \delta(y-y_p) \delta(z-z_p) \quad (3)$$

where I is the current in Ampere specific to a point in Cartesian $x-y-z$ space by the Dirac delta function, x_p , y_p and z_p are the source location coordination. By combining eqs. 2 and 3 into eq. (1), this will be produced:

$$\nabla \cdot [\sigma \nabla \phi_{(x,y,z)}] = -I \delta(x-x_p) \delta(y-y_p) \delta(z-z_p) \quad (4)$$

After discretizing eq. (4) as it is explained in the Dey and Morrison (1979) this will be the outcome:

$$C \phi = S \quad (5)$$

where C is the $LMN \times LMN$ matrix, called the capacitance matrix with function of the geometry, which is the physical property distribution in the grid, and S is a vector of numeric value of the current electrode (injected current value in Amperes) in each node where LMN is the three dimension of the resistivity cube ($L \times M \times N$). S is a vector and shows position of current electrodes the value of $+1$ on the location of the injection electrode, and -1 for the position of sink electrode, and after calculation of all potentials on the nodes, multiply the result by the real injected current for the operation simplicity. To calculate the electrical potential matrix in each configuration for S , the C matrix should be inverted which is not an easy process. As the current vectors have to pass through resistors, they have to pass through the surface of a cube.

2.2. Modeling by the calculation of the Kirchhoff's Law

Modeling by the calculation of the Kirchhoff's Law helps us to discretize the problem in an easier way to get the voltage distribution which is the traditional method for calculating ϕ in eq. (5). According to this method, the cube should be disassembled to six surfaces, and after solving C matrix assembled back to calculate the model response as shown in Fig. 2. Then based on survey configuration, model response will be calculated. In the new method, a resistor network model is assumed to be similar to the resistivity model. As each surface in traditional model has only one value, the resistor model is shifted by half a surface to make both models more similar. As in earlier methods, potential values are assigned to the center, whereas in this method potential values are assigned to the edges. By this assumption each resistor is assumed to connect the center of a surface to the vicinity surface in each direction. As these two surfaces may have different values, then the equivalent resistor value is assumed to be the value of the left surface, top or front surface for each direction, and this rule should apply to

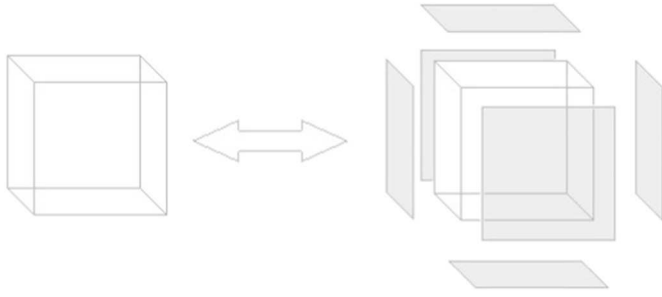


Fig. 2. One cube disassemble.

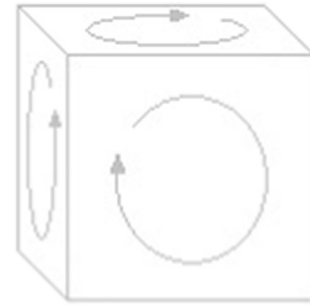


Fig. 3. Current direction.

the whole model as shown in Fig. 1. As these two models have different units, it assumes a unit value for distance (e.g. 1 m as it is suggested in Loke et al. (2014b)), and converts resistivity with ohm-meter unit to resistor with ohm unit. After these assumptions, the voltage distributions as well as the sensitivity matrix, are similar on both models. It will be discussed in the following section. This will help to model the problem physically using the resistor network by solving 3D resistor network. The two steps are combined to calculate voltage distribution which reduces the calculation process, however, the matrix is not symmetrical anymore. Another advantage of this method is increasing accuracy when singularity is removed (Lowry et al., 1989). In this method, no singularity will be created from the current electrode position, while in earlier methods the singularity needs to be removed with the different techniques as Zhao and Yedlin (1996). This feature not only increases the accuracy but also reduces the calculation time. As this method is not sensitive to current electrode location, therefore it could be used for voltage distribution calculation of any possible conventional (Schlumberger, Wenner, Pole-Pole, Dipole-Dipole, ...) or any unconventional electrode configurations which are used for optimization purposes Wilkinson et al. (2006), Wilkinson et al. (2012), Loke et al. (2010) and Loke et al. (2010). If a resistor network is assumed with $m \times n \times k$ dimensions, then number of nodes and edges will be:

$$\text{nodes} = (m + 1) \times (n + 1) \times (k + 1) \quad (6)$$

$$\text{edges} = (((m \times (n + 1)) + (n \times (m + 1))) \times (k + 1)) + ((m + 1) \times (n + 1) \times k) \quad (7)$$

And finally,

$$\text{surfaces} = (m \times n \times (k + 1)) + (k \times n \times (m + 1)) + (m \times k \times (n + 1)) \quad (8)$$

The final matrix will be the inverse of a square matrix with the number of rows and columns equivalent to the number of edges. There are two types of Kirchhoff's Law, but as they both act on edges, they can be combined in a system of linear equations and ordered as a set to be prepared for calculation. KCL is about all nodes which means current summation in each node is zero except for those nodes which are source of injection or sink. For injection value +1 or -1 for sink is allocated. But as this current is a relative value, the equation can be solved with one injection or sink only, and for pair electrodes (injection and sink) would be the summation of two answer matrices. KVL is algebraic sum of voltage distribution in each loop which is zero. As the 3D resistor network is a wired cube, in this method KVL is applied to all three directions of current loops as shown in Fig. 3. On each surface current, is assumed in clockwise direction in plan view. if the calculated current result from equation gets a negative value, it means the current direction is in the opposite direction as per Newton Raphson method for solving current method, which is explained by Cilliers et al. (2001). A more detailed look on the resistor network, shows that some edges contribute in all three dimensional surfaces, only if they are not placed in

the edge surfaces. Repeating these edges in the main matrix leads us to the matrix rows which is singular. To solve this problem, one can keep a counter on edges and any equation which exceeds edge counter >4 times, should be neglected. But in this method, all surfaces from $m \times n$ dimensions and $m \times k$ dimensions were used, and $n \times k$ dimensions were not included which provides a square matrix with no singularity because it prevents the repetition of red edges in Fig. 5.

2.3. Matrix formulation

For matrix formulation, two Kirchhoff's Laws should be applied to the resistor network. The first Kirchhoff's Law is Kirchhoff's Current Law (KCL), which is applied to each node of the resistor network.

$$\sum I_{\text{node}} = I_{\text{injection}} \delta(r - r_s) \quad (9)$$

This law is a charge conservative law and states that, in every node, the numerical summations of currents are zero. When a charge is injected into a node, it should be indicated as an injection node which is the condition for the second law of Kirchhoff (KVL), which explains that in each loop, the summation of voltages is zero as shown in Fig. 4.

$$\sum V_{\text{loop}} = \sum_{i=1}^l I_i R_i = 0 \quad (10)$$

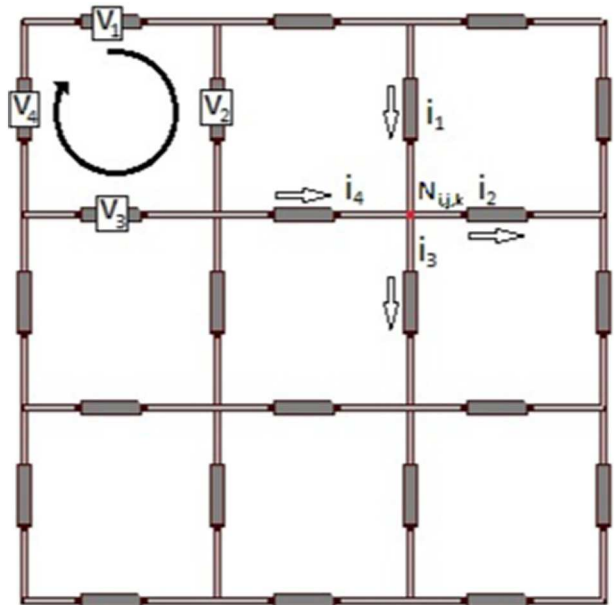


Fig. 4. 2D resistor network.

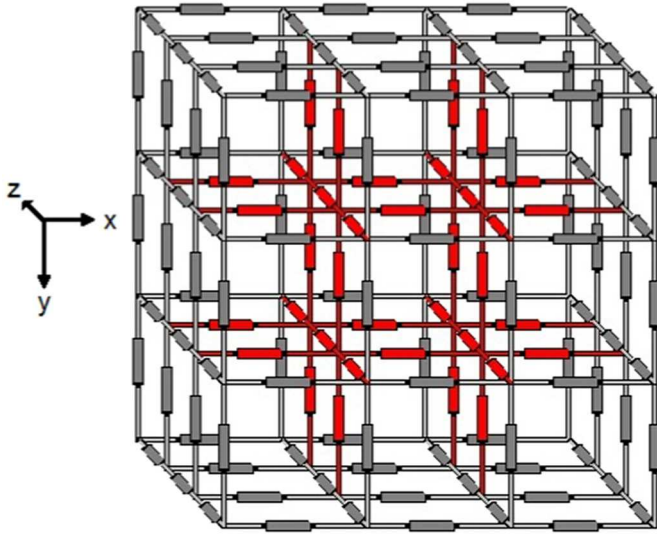


Fig. 5. 3D resistor network.

This equation can also be rewritten for any surfaces in Fig. 4 or Fig. 5 for all surfaces in any possible direction or surface size but here it is considered only in three dimensions and only one surface wide. A capacitance matrix will be formed by applying these two equations for each node and loop. Then, as the combined number of nodes and loops exceeds the number of edges, some of the equations should be omitted for the common edges between many surfaces to avoid matrix singularity. These common edges are shown as red in Fig. 5.

2.4. Boundary conditions

In the Electrical Resistivity (ER) method a mixed boundary condition is used:

$$\alpha(x, y, z)\phi(x, y, z) + \beta(x, y, z)\frac{\partial\phi(x, y, z)}{\partial\eta} = 0 \quad (11)$$

Where $\phi(x, y, z)$ is the voltage, $\alpha(x, y, z)$ and $\beta(x, y, z)$ are general functions in solving partial differential equations with these conditions, $\alpha(x, y, z) \geq 0$, $\beta(x, y, z) \geq 0$ and $\alpha + \beta > 0$.

$\alpha(x, y, z)$, $\beta(x, y, z)$ are unit-less, and as the solved network is considered cubical, they will have values only when a surface is connected to the next surface via a resistor. Eq. (11) is achieved in the boundary conditions after applying the Kirchhoff's Law. During matrix formulation, when a node is not placed in the middle, applying the Kirchhoff's Law will invoke the boundary conditions. If a node has no vicinity node in any direction, then the current will be 0; this is the Dirichlet boundary condition $\alpha(x, y, z)\phi(x, y, z) = 0$. Also, all currents have to pass through resistors, satisfying the Neumann boundary condition $\frac{\beta(x, y, z)\partial\phi(x, y, z)}{\partial\eta} = 0$.

This boundary condition is used in traditional modeling but as in this modeling method 3D resistor network is used, boundary condition is applied on the borders as current cannot pass them due to physical limitation. This boundary condition is comparable to the tank model in Res3DMOD software (Geotomo Software, Malaysia) Loke et al. (2014b), where the tank has isolated boundaries. Unlike in real survey, current cannot pass beyond the model. To overcome this limitation, model can expand for limited surfaces in each dimensions, for instance three surfaces in each, especially with greater values for resistor. This type of boundary condition will increase the sensitivities over the edges in comparison to the traditional method.

2.5. Building the matrix model

A matrix model is defined as the $m \times n \times k$ dimensions of a resistor network. Each inner node is connected to six other nodes, one in each direction (as shown in the red area of Fig. 5. Boundary nodes are restricted from one or more sides, so they include fewer edges.

First, a cube will be created with $m \times n \times k$ dimensions, in which m represents the x direction, n is z and k is y. For 2D purposes, k can be zero but m or n must be equal to or >1 . The main calculation will be based on calculating the current on each edge by using eqs. 9 and 10. A matrix will be created including:

$$\mathbf{A} \mathbf{I} = \mathbf{S} \quad (12)$$

in which \mathbf{I} is a vector for current on each edge, and \mathbf{S} is a vector to show where the current injection is placed. Matrix \mathbf{A} is defined below:

$$\mathbf{A} = \begin{bmatrix} \sum \mathbf{I}_i \\ \dots \\ \sum \mathbf{I}_i \mathbf{R}_i \end{bmatrix} \quad (13)$$

Matrix \mathbf{A} is a combination of two matrices. The one at the top is the summation of all the currents to a node and it follows with the summation of voltages in each loop. As the number of nodes are less than loops, the rest of columns are filled with null values. Furthermore, for all loops the summation of voltages will be zero and the equivalent row in \mathbf{S} matrix is zero. Also for all nodes except sink or source nodes the summation of all incoming and outgoing currents at the node is zero. Resistor values are known in the model, and voltages on each node must be calculated. For solving the 3D resistor network, it is obvious that based on eqs. 6, 7 and 8, more equations than unknowns will be available; this will cause the singularity problem in solving eq. (12). As shown in Fig. 5, red edges are common between different surfaces in the XY, XZ and YZ directions. To overcome this problem, common edges must be omitted from equations in the KVL section in eq. (13). A matrix in eq. 13 is a square matrix when each dimension is as long as the edge number. The relationship between the edges, nodes and surfaces is defined as below:

$$\text{edges} = \text{surfaces} + \text{Nodes} - 1 \quad (14)$$

After solving eq. (12), all edge currents are solved, so based on that, $\nabla V_i = I_i R_i$ will be calculated with the solved I_i and known resistor value

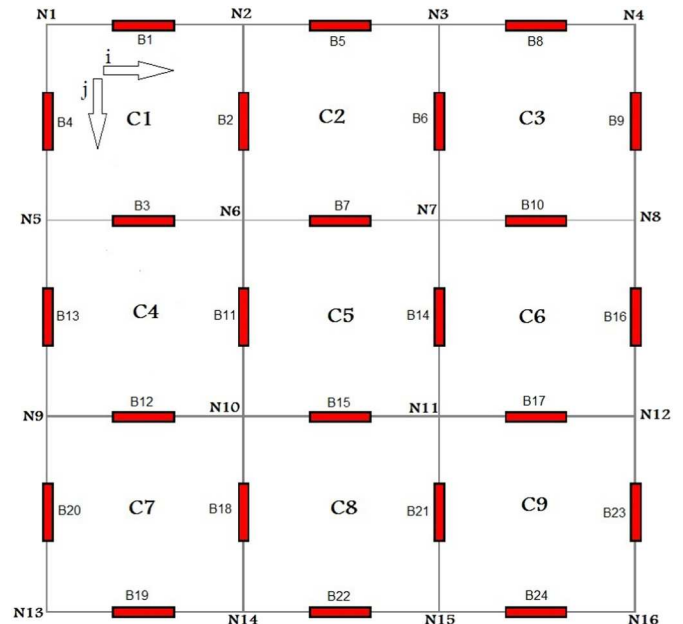


Fig. 6. Resistivity network 3 × 3.

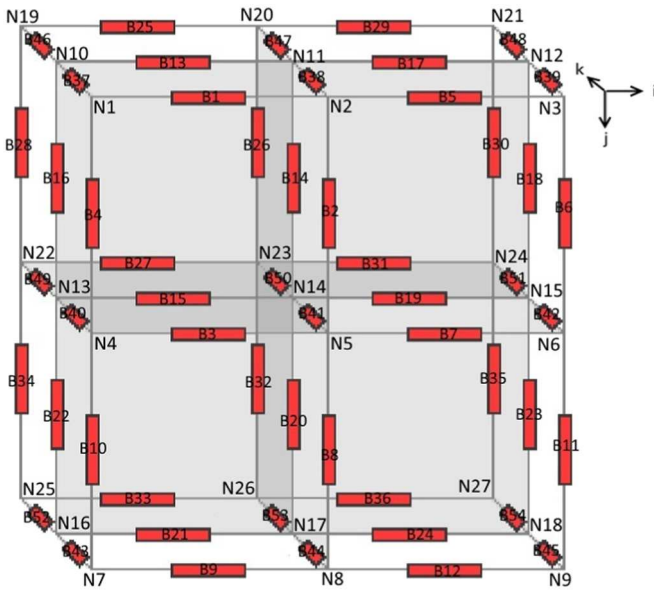


Fig. 7. Resistivity network 2x2x2 highlighted all surfaces which share N14 node.

R_i accordingly. Finally, a vector of V will be obtained after this calculation.

Another important point is that for a complete calculation, all possible survey points in the surface should be calculated, for instance, XY surface in a 3D section and X surface in 2D. After calculating all possible points for injecting current in eq. (13) in the KCL section, the corresponding S will be 1 which is refer to injection source. To calculate

sink source matrix, simply needed to multiply an injection source matrix results by -1 . For instance for calculation of a dipole (which normally is used in resistivity modeling), it can calculate two sources and turn on of them to sink and numerically add two matrices. Then for calculating the voltage between two nodes, these two calculated voltages must be subtracted; the value must be multiplied by the real current value, as it was assumed to be 1.

$$V_{MN} = V_M - V_N \quad (15)$$

2.6. Solving a sample 2D resistor network

In 2D resistor network model, there are i and j directions as shown in Fig. 6. There are 9 surfaces, 16 nodes and 24 edges. These numbers can be calculated from formulas 6,7 and 8 when m and n are equal 3 and k is equal to 0. At the start all nodes will be numbered in i direction and then continued in j direction (left to right then top to bottom) as shown in Fig. 6. Similarly, this sequence is repeated for assigning numbers to each surface. Edges numbers are based on each surface, starting from minimum surface, and node number in the surface in a clockwise direction. Each edge will be encountered only once on the first surface it was presented. Each edge is indicated as a resistor, so to model an anomaly, the resistor value of an edge could be changed. Nodes will be where the current source (or sink based on polarity) is placed. As in geoelectric, current electrodes are on the surface, only nodes N1-N4 will be considered as current sources. However, in case of borehole study, long electrode study or any lab models any nodes (from N1-N16) could be a source. Long electrode in this approach, is simulated as a resistor with 0Ω resistivity.

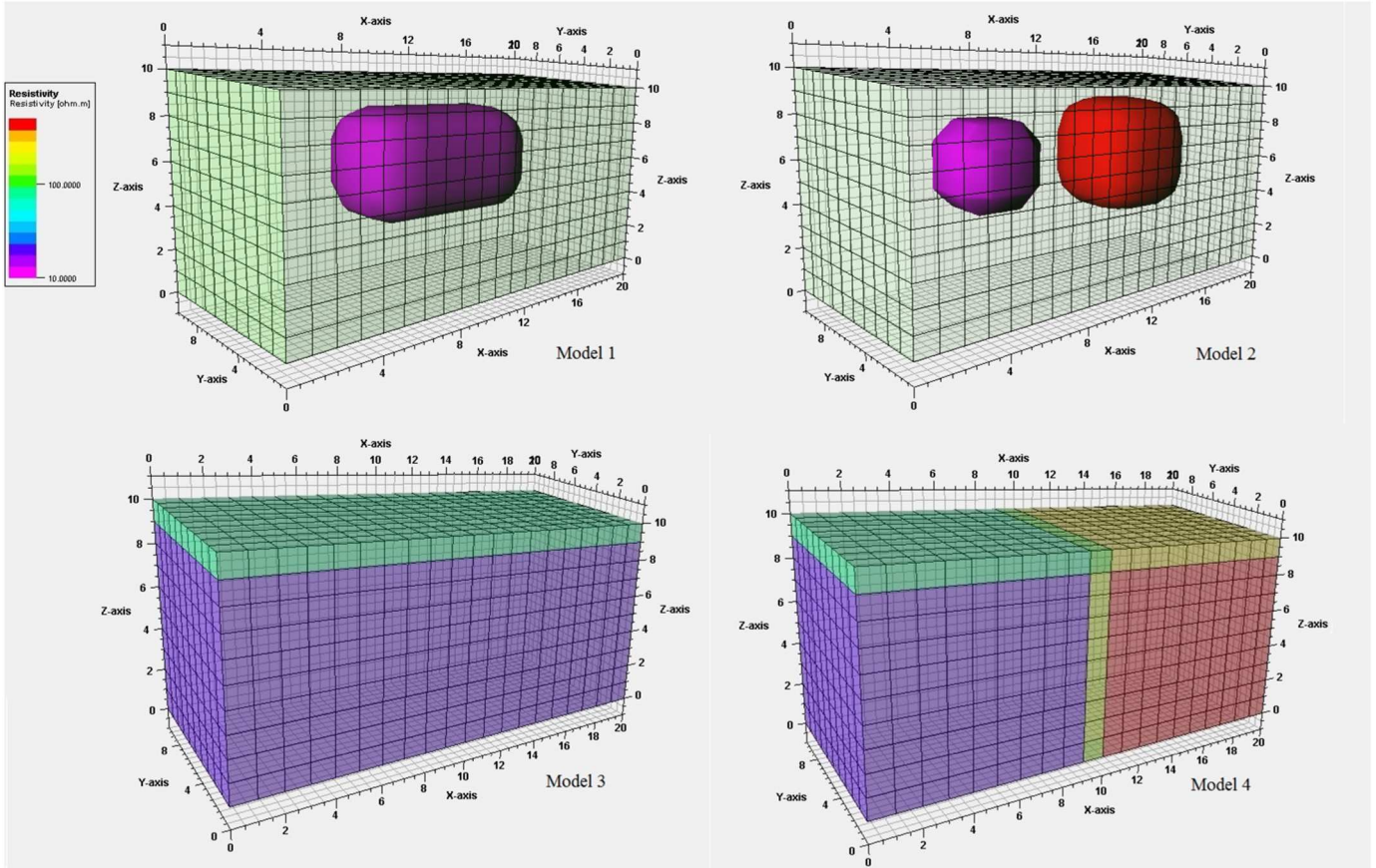


Fig. 8. Resistivity model, four base model.

it is explained in the section on solving 2D resistor network section, the **A** matrix will be used with all different current source combination (**I** matrix), and the result will be a matrix with voltage difference on each single edge. Solving a 3D case is very similar to 2D except the edges in *jk* direction (Fig. 7) will not participate in **A** matrix as they are calculated in *ij* and *ik* processes.

$$A_{KVL}(\text{surface } 1) = [100, 100, -100, -100, \dots, 0] \quad (22)$$

An example for formation of a KVL matrix is shown in eq. (22). This matrix shows the KVL equation on the surface 1 which is enclosed by N1,N2,N4 and N5. In A_{KVL} matrix 17 all values (100) define the value for an edge resistor (by their position in the matrix) with current passing through the resistor in the same way which is assumed; All negative values define a resistor with current passing through that resistor in the opposite direction. All horizontal

currents from left to right are considered positive in the Fig. 7. For instance current from N1 to N2 is positive (B1 in Fig. 7) while from N5 to N4 (B3 in Fig. 7) is negative.

Also all currents from top to bottom direction are positive and they are negative in the opposite direction. For example, in surface 1 in Fig. 7 current from N2 to N5 (Fig. 7) is positive while current from N4 to N1 is negative. Based on their position, each edge could have negative or positive current. For instance, B2 (in Fig. 7) in surface 1 has positive value, but in surface 2 the same edge has negative value. Solving resistor network using this method is only one step solution without any singularity involved. Also shape of 3D resistor network could change. This helps building model in any shape to resemble topography. Furthermore value for any edge will help to make a model in any possible shape or resistivity distribution. This method will be suitable for studying any kind of anomaly or topography as well as any kind of electrode configuration, in both conventional or non conventional methods.

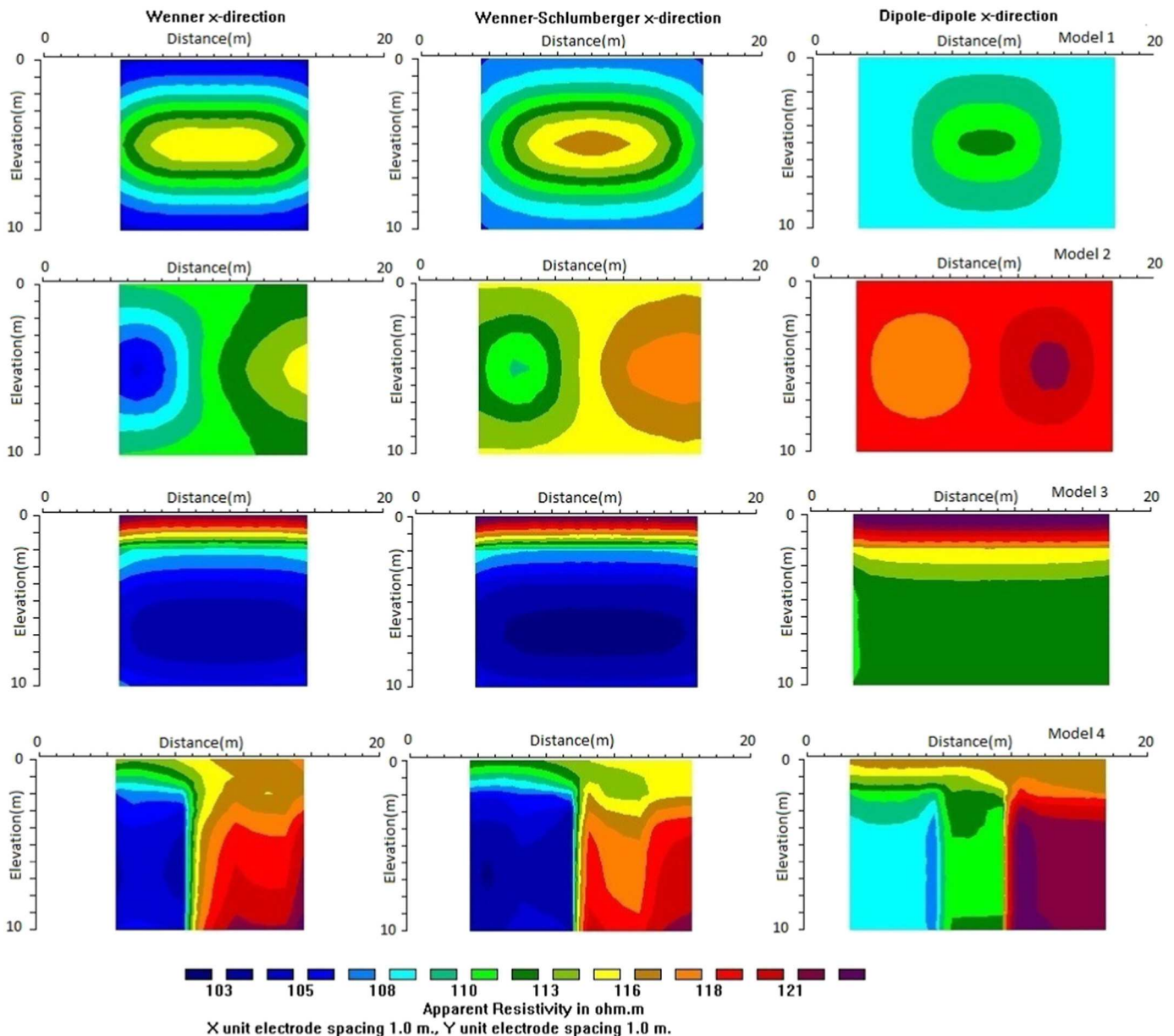


Fig. 9. Resistivity model, model response with $a = 3$.

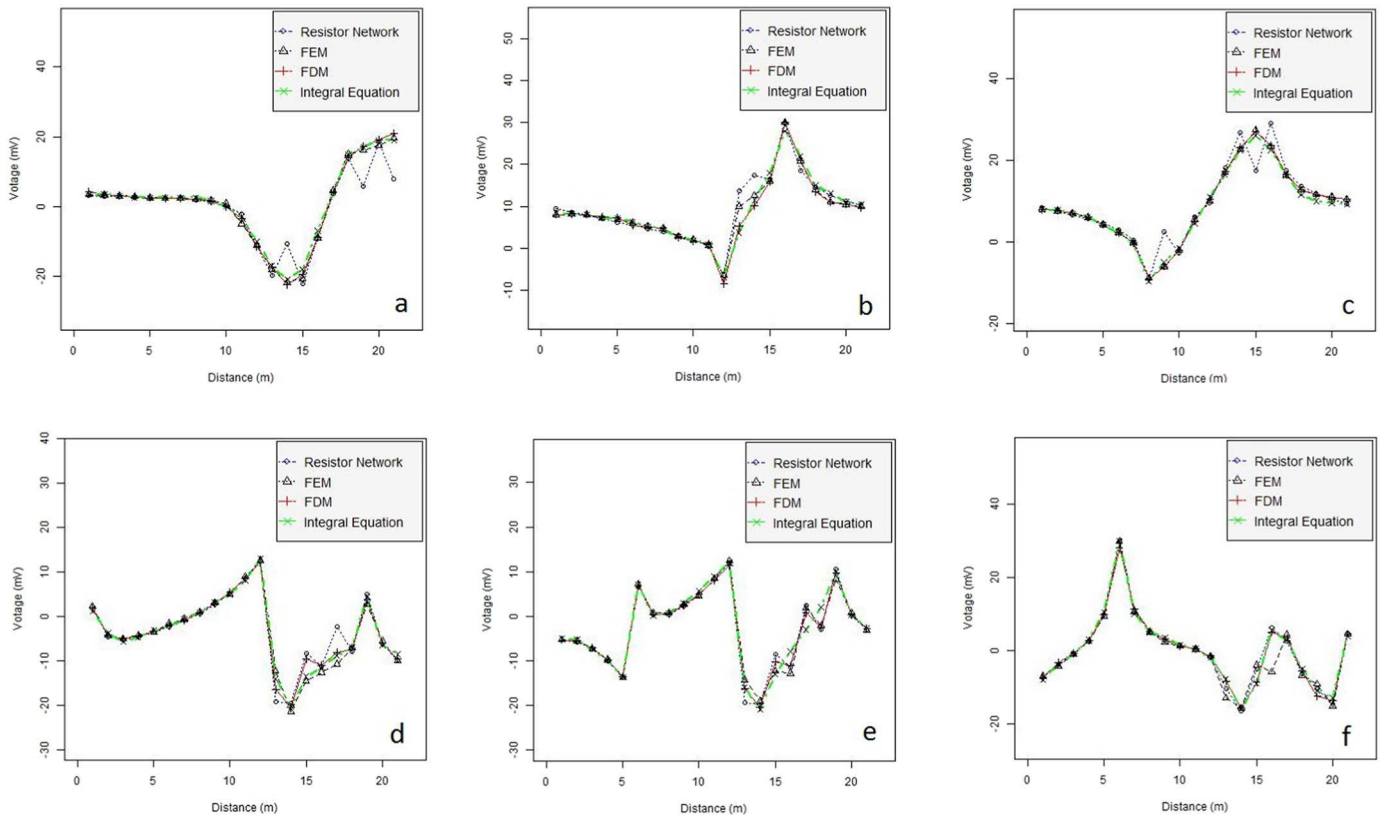


Fig. 10. Cross section model 2, a. profile on quarter distance from the start point in x direction, b. profile in the x direction in the middle, c. profile in the x direction on third quarter from the start point, d. profile on quarter distance from the beginning in the y direction, e. profile in the middle of the model in the y direction, f. profile in the third quarter distance from the beginning in the y direction.

3. Model computations

3.1. Synthetic model computation

The **A** matrix in Eq. (12) is composed of two main matrices. In [Dey and Morrison \(1979\)](#) this matrix discretized as six surfaces and is solved using FDM (Finite Difference Method). [Sasaki \(1994\)](#) solved the partial differential equation using FEM (Finite Element Method). In this paper the solution approach is totally different from either techniques. The main matrix is divided into two parts, in which the first part is based on KCL and the second part is based on KVL. KCL equations are related to node numbers while KVL equations are related to edge numbers. There are some critical edges in which the related surfaces must be omitted in the KVL matrix. These surfaces make the edges repeat more than it is necessary, and make the matrix non-invertible, which are marked in red in [Fig. 5](#).

3.2. Model result

Results from synthetic data from a couple of user defined 3D model are represented. A couple of Alpha models are selected with spacing of 1 m ([Loke et al., 2010](#)). The models together with their pseudosection for the Wenner array are shown in [Fig. 8](#) and [Fig. 9](#). The apparent resistivity values are calculated for these models using Finite Difference forward modeling Tank model with RES3DMOD for comparison. Wenner method, Schlumberger method, and dipole-dipole method were used for comparison between model response and RES3DMOD software.

Then the same model is created using 3D resistor network, and same array configurations are calculated using the same method as shown in [Fig. 8](#). As the spacing (which is called 'a') is set to 1 m, same value for resistors (with Ω unit) are used as resistivity network (with Ω -meter

unit). Wenner and dipole-dipole methods are used for test and comparison of data from traditional method and the new method. In all cases, the 'a' for those methods were set from 1 to 5, and factor values from 1 to 9 ([Loke et al., 2010](#)). The model in this paper used for synthetic data is comprised of $20 \times 10 \times 10$ cubes, which gives $21 \times 11 \times 11$ nodes. Boundaries of tank value were set at the edge of the model, and intervals in all directions were assumed as 1.0 m. All models are calculated in x direction for Wenner, Wenner-Schlumberger and dipole-dipole with RES3DMOD software for comparison. Also, contour values are chosen in logarithmic intervals.

For calculation of different array configuration on the new modeling approach, **S** in Eq. (12) set for each node on the surface and the voltage distribution calculated. Then, an array of matrices produced where each one represented as an array configuration position. If it is needed to calculate a Wenner array for instance, we get the matrix on the injection and sink electrodes index chosen, and subtracted to calculate voltage on each node. Voltage difference calculated on potential electrodes for this single acquisition. In other words, the model result for each node with the current source applied, will be a vector of voltage. In addition to the resistivity matrix, this vector can be used for the calculation of a sensitivity matrix for inversion purposes. Also, the voltage is calculated in each node. So, for calculating an array response, one should assume that current electrodes are placed at A and B positions. If the potential electrodes are M and N, to calculate V_{MN} Eq. (12) should be solved, and the corresponding KCL row should be assigned +1 for the current source and -1 for current sink. After solving the equation the answer is multiplied by the real current value in Ampere, and result which is V_{MN} will be in Volt. The same procedure will be repeated for electrode B. Then, there are two voltage vectors, results of these operations, which must multiplied by the real injected current value.

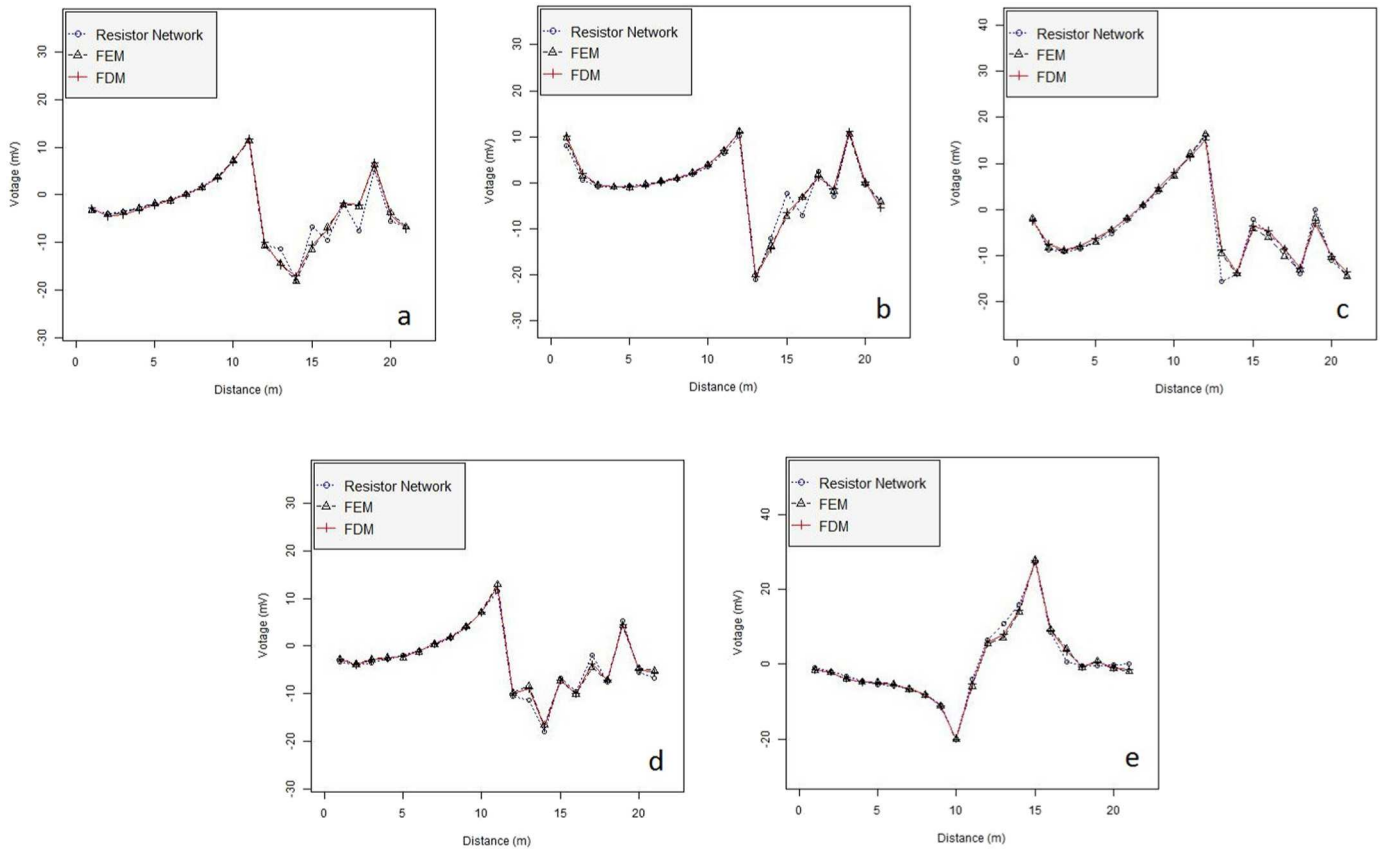


Fig. 11. Cross section model 1,3 and 4, a, profile in the middle of model 1 in x direction, b, profile in the middle of model 1 in y direction, c, profile in middle of the model 3 in the x direction, d, profile in middle of the model 3 in the y direction, e, profile in middle of the model 4 in the x direction.

3.3. Method comparison on experimental data

In this section, the results from a calculated data set for four models with $20 \times 10 \times 10$ blocks will be presented. The electrode spacing is one meter in i and j directions. All four models described in the previous section were solved with resistor network method, Finite Element Method (FEM) and Finite Difference Method (FDM). To compare the results of these three methods, at the first step, the voltage output for FEM and FDM is normalised for 1.0 m electrode spacing. Then a profile is selected, which is in the middle of the model ($Y = 5$). The injection electrodes are placed on nodes 5 and 10 in X direction as shown in Fig. 10 and Fig. 11.

In Fig. 10 model 2 is presented, it includes three profiles in x direction (a,b and c) and three profile in y direction (d,e and f). Subplot a and d are a quarter from the model corner, which a is in x and subplot d is in y direction. Subplot b in the middle of the model in x direction when subplot e is similar but in y direction, finally subplot c and f are three quarter of model from beginning when c is in x direction and subplot f is in y direction.

In Fig. 11 the other three models are presented. Subplot a is middle of model 1 profile in x direction when subplot b is similar but in y direction. Subplot c is middle of model 3 profile in x direction when subplot d is similar but in y direction. Finally subplot e is middle of model 4 profile in x direction.

These results show that in different methods, model response in general is close. However, there are two reasons to cause a sudden change or spike in the results. The first reason is the different methods' gridding, and normalizing the result for 1.0 m interval to match the results. The second reason is the rate of the changes which is a cube in FEM and FDM and a resistor network in the current method.

The FEM and FDM models are modeled as tank models to resemble the limited boundary condition in the resistivity network model

Loke et al. (2014b). As the current electrodes placed on nodes 5 and 10 for calculation of different voltage in the given models, the significant voltage changes occurred above the context property changes in depth.

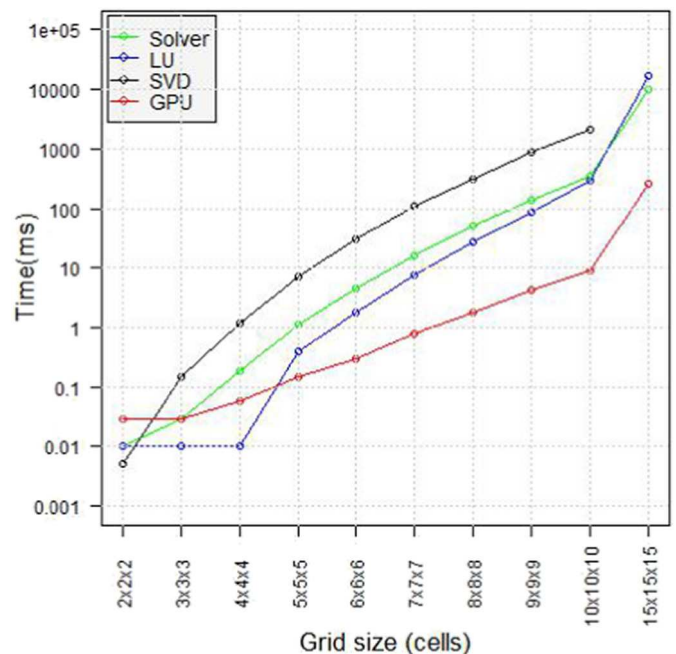


Fig. 12. Speed comparison for different solving methods.

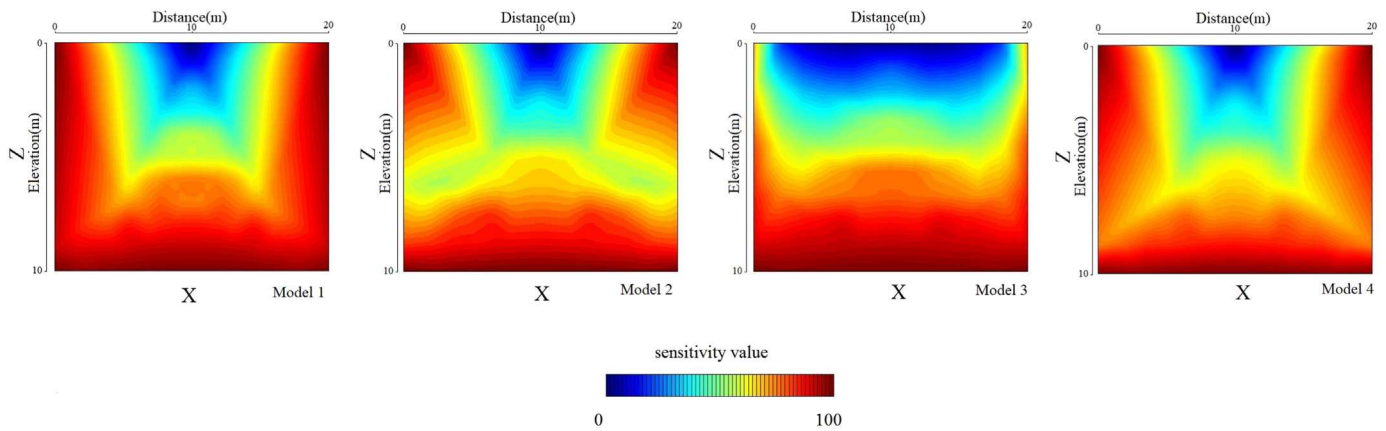


Fig. 13. Sensitivity comparison between 3D resistivity model and mathematical model.

3.4. Performance of the algorithm

Three different solvers are used in this article. The first method was a simple matrix solver (Gaussian elimination) which is called "RN solver" (RN stands for Resistor Network). Also, the same method was developed to solve the matrix by using GPU³ which is called "GPU method" in this paper. In addition to the GPU method, a library called NMath is used for comparison purpose with the following solution methods:

- LU
- QR
- SVD
- Gram-Schmidt

The last method uses parallel computing through a computer graphic card and graphics processing unit to solve the matrix Farber (2011).

3.4.1. Speed

The computer used to acquire these data was a M4600 DELL with 32GB RAM and NVIDIA 1GB Graphic RAM, 3.4 GHz CPU speed. Fig. 12 different speeds are compared in different methods, as QR and Gram-Schmidt method results were near to LU and SVD, they were not graphed in the figure; all units are in milliseconds.

This figure shows that for small data sets, the GPU method is slower, but when the data size is increased, this approach is exponentially faster than the other methods. As this solution is based on GPU and parallel computation, it obviously benefits from running on any parallel computer or supercomputer.

3.4.2. Accuracy

An assembly of a physical model using the resistor network is quick and easy. Two arrays with 10x10x10 and 5x5x5 dimension are created, to test the GPU method against the physical model. The calculated response was accurate up to 0.1 V with lab equipment. Boundary conditions in this method are profoundly different from the mixed boundary conditions that are used in geo-electrical modeling. The boundary condition is very similar to the tank model found in the geo-electrical experimental lab. In this method, the sensitivities on the borders and edges are higher than the model in the field (Fig. 13). In order to make the result more realistic and similar to field data, the 3D resistivity model could be assumed to be bigger in the x and y directions (for instance, 3 surfaces in each direction) and all boundaries could be assumed to have zero voltage. Fig. 13 shows the differences between

the 3D resistor network method and the model sensitivity calculated mathematically.

4. Conclusion

A new modeling technique has been successfully developed. This method enables 2D and 3D modeling on resistivity anomalies. By using this technique, any model could be converted to a resistor network. This method is based on discretizing a resistor network using the Kirchhoff's Law in which helps removing singularity of the model. No assembling or disassembling procedure is needed in this method, which decreases modeling complexity. This method presents a fast and robust way to calculate the potential distribution in the resistor network. Simulating topography, long electrodes and borehole study are possible with this method by changing the resistor values or the potential electrodes placement in the model. This method could be used for analyzing the result and sensitivity of any electrode configuration. This approach could be used in both conventional and unconventional optimization survey designs. This method shows more accuracy in the center of the model in comparison with the FD and the FEM. The parallel processing technique which is used to solve the resistor network model enables this method to be faster when data size increases.

Acknowledgment

This paper is a part of my PhD research in UTP (University Teknologi Petronas), and I would like to express my special appreciation and thanks to my supervisors Professor Dr. Deva Ghosh and Professor Dr. Loke. I would like to acknowledge UTP for allowing me to publish this paper externally.

References

- Bin, Z., Greenhalgh, S., 2001. Finite element three dimensional direct current resistivity modelling: accuracy and efficiency considerations. *Geophys. J. Int.* 145 (3), 679–688.
- Cilliers, J.J., Xie, W., Neethling, S.J., Randall, E.W., Wilkinson, A.J., 2001. Electrical resistance tomography using a bi-directional current pulse technique. *Meas. Sci. Technol.* 12 (8):997 URL <http://stacks.iop.org/0957-0233/12/i=8/a=302>.
- Coggon, J., 1971. Electromagnetic and electrical modeling by the finite element method. *Geophysics* 36 (1), 679–688.
- Dahlin, T., Zhou, B., SEP 2004. A numerical comparison of 2d resistivity imaging with 10 electrode arrays. *Geophys. Prospect.* 52 (5), 379–398.
- Dey, A., Morrison, H.F., 1979. Resistivity modeling for arbitrarily shaped three-dimensional structures. *Geophysics* 44 (4):753–780. <http://geophysics.geoscienceworld.org/content/44/4/753.abstract>.
- Dieter, K., Paterson, N.R., Grant, F.S., 1969. Ip and resistivity type curves for three dimensional bodies. *Geophysics* 34 (4):615–632. <https://doi.org/10.1190/1.1440035>.
- Farber, R., 2011. *CUDA Application Design and Development*. Elsevier.
- Hvozdar, M., Kaikkonen, P., 1998. An integral equations solution of the forward d.c. geoelectric problem for a 3-d body of inhomogeneous conductivity buried in a halfspace. *J. Appl. Geophys.* 39 (2):95–107. <http://www.sciencedirect.com/science/article/pii/S092698519800007X>.

³ Graphics Processing/Processor Unit

- Lee, T., 1975. An integral equation and its solution for some two-and three-dimensional problems in resistivity and induced polarization. *Geophys. J. R. Astron. Soc.* 42 (1): 81–95. <https://doi.org/10.1111/j.1365-246X.1975.tb05851.x>.
- Li, Y., Spitzer, K., 2002. Three-dimensional dc resistivity forward modelling using finite elements in comparison with finite-difference solutions. *Geophys. J. Int.* 151 (3): 924–934. <http://gji.oxfordjournals.org/content/151/3/924.abstract>.
- Loke, M., Dahlin, T., MAR 2002. A comparison of the gauss-newton and quasi-newton methods in resistivity imaging inversion. *J. Appl. Geophys.* 49 (3), 149–162.
- Loke, M., Wilkinson, P., Chambers, J., 2010a. Fast computation of optimized electrode arrays for 2d resistivity surveys. *Comput. Geosci.* 36 (11):1414–1426. <http://www.sciencedirect.com/science/article/pii/S0098300410002128>.
- Loke, M.H., Wilkinson, P.B., Chambers, J.E., 2010b. Parallel computation of optimized arrays for 2-d electrical imaging surveys. *Geophys. J. Int.* 183 (3), 1302–1315.
- Loke, M., Wilkinson, P., Chambers, J., Strutt, M., 2014a. Optimized arrays for 2d cross-borehole electrical tomography surveys. *Geophys. Prospect.* 62 (1), 172–189.
- Loke, M.H., Wilkinson, P.B., Uhlemann, S.S., Chambers, J.E., Oxby, L.S., 2014b. Computation of optimized arrays for 3-d electrical imaging surveys. *Geophys. J. Int.* 199 (3): 1751–1764. <http://gji.oxfordjournals.org/content/199/3/1751.abstract>.
- Lowry, T., Allen, M.B., Shive, P.N., 1989. Singularity removal: a refinement of resistivity modeling techniques. *Geophysics* 54 (6):766–774. <https://doi.org/10.1190/1.1442704>.
- Ma, Q., 2002. The boundary element method for 3-d dc resistivity modeling in layered earth. *Geophysics* 67 (2):610–617. <https://doi.org/10.1190/1.1468622>.
- Martorana, R., Fiandaca, G., Ponsati, A.C., Cosentino, P.L., MAR 2009. Comparative tests on different multi-electrode arrays using models in near-surface geophysics. *J. Geophys. Eng.* 6 (1), 1–20.
- Mufti, I.R., 1976. Finite-difference resistivity modeling for arbitrarily shaped two-dimensional structures. *Geophysics* 41 (1), 62–78.
- Penz, S., Chauris, H., Donno, D., Mehl, C., 2013. Resistivity modelling with topography. *Geophys. J. Int.* 194 (3):1486–1497. <https://doi.org/10.1093/gji/ggt169>.
- Plattner, A., Maurer, H.R., Vorloeper, J., Blome, M., APR 2012. 3-d electrical resistivity tomography using adaptive wavelet parameter grids. *Geophys. J. Int.* 189 (1), 317–330.
- Rucker, D.F., Loke, M.H., Levitt, M.T., Noonan, G.E., 2010. Electrical-resistivity characterization of an industrial site using long electrodes. *Geophysics* 75 (4):WA95–WA104. <https://doi.org/10.1190/1.3464806>.
- Sasaki, Y., FEB 1989. Two-dimensional joint inversion of magnetotelluric and dipole-dipole resistivity data. *Geophysics* 54 (2), 254–262.
- Sasaki, Y., 1994. 3-d resistivity inversion using the finite element method. *Geophysics* 59 (12):1839–1848. <https://doi.org/10.1190/1.1443571>.
- Spitzer, K., 1995. A 3-d finite-difference algorithm for dc resistivity modelling using conjugate gradient methods. *Geophys. J. Int.* 123 (3):903–914. <http://gji.oxfordjournals.org/content/123/3/903.abstract>.
- Wang, T., Fang, S., Mezzatesta, A., Jul 2000. Three-dimensional finite-difference resistivity modeling using an upgridding method. *Geoscience and Remote Sensing. IEEE Transactions on* 38 (4), 1544–1550.
- Wilkinson, P.B., Meldrum, P.I., Chambers, J.E., Kuras, O., Ogilvy, R.D., 2006. Improved strategies for the automatic selection of optimized sets of electrical resistivity tomography measurement configurations. *Geophys. J. Int.* 167 (3):1119–1126. <https://doi.org/10.1111/j.1365-246X.2006.03196.x>.
- Wilkinson, P.B., Loke, M.H., Meldrum, P.I., Chambers, J.E., Kuras, O., Gunn, D.A., Ogilvy, R.D., APR 2012. Practical aspects of applied optimized survey design for electrical resistivity tomography. *Geophys. J. Int.* 189 (1), 428–440.
- Xu, S.-Z., Zhao, S., Ni, Y., 1998. A boundary element method for 2-d dc resistivity modeling with a point current source. *Geophysics* 63 (2), 399–404.
- Zhang, J., Mackie, R., Madden, T., 1995. 3-d resistivity forward modeling and inversion using conjugate gradients. *Geophysics* 60 (5):1313–1325. <https://doi.org/10.1190/1.1443868>.
- Zhao, S., Yedlin, M.J., 1996. Some refinements on the finite difference method for 3-d dc resistivity modeling. *Geophysics* 61 (5):1301–1307. <https://doi.org/10.1190/1.1444053>.